

# Dominance of pollutant aerosols over an urban region and its impact on boundary layer temperature profile

Shamitaksha Talukdar<sup>1</sup>, Soumyajyoti Jana<sup>1</sup> and Animesh Maitra<sup>1\*</sup>,

<sup>1</sup>*S. K. Mitra Centre for Research in Space Environment*

*Institute of Radio Physics and Electronics, University of Calcutta*

*Kolkata 700 009, India*

**[shamitaksha@gmail.com](mailto:shamitaksha@gmail.com), [mantu.abc@gmail.com](mailto:mantu.abc@gmail.com), [animesh.maitra@gmail.com](mailto:animesh.maitra@gmail.com)**

## Corresponding Author:

Animesh Maitra,

Professor, Institute of Radio Physics and Electronics and

Director, S. K. Mitra Centre for Research in Space Environment,

University of Calcutta,

92, Acharya Prafulla Chandra Road,

Kolkata -700009, India.

Tel +91-33-2350-9116 (Extn 28) (Office)

Fax +91-33-2351-5828

Email [animesh.maitra@gmail.com](mailto:animesh.maitra@gmail.com)

[am.rpe@caluniv.ac.in](mailto:am.rpe@caluniv.ac.in)

This article has been accepted for publication and undergone full peer review but has not been through the copyediting, typesetting, pagination and proofreading process which may lead to differences between this version and the Version of Record. Please cite this article as doi: 10.1002/2016JD025770

## Key Points:

- **Dominance of pollutant particles over urban region affects temperature lapse rate**
- **Growth of convection in the lower troposphere is notably affected on pollutant dominating days**
- **Transported air masses significantly influence the spectral pattern of single scattering albedo**

## Abstract

Collocated measurements of aerosol optical depth (AOD) and black carbon (BC) at different wavelengths over Kolkata, an urban region in eastern India, have been used to calculate aerosol single scattering albedo (SSA). The wavelength dependence of SSA and AOD has been presented to discriminate the aerosol types over this highly populated metropolitan area. The spectral pattern shows that SSA decreases with wavelength for most of the time in a year and corresponding Angstrom coefficient is greater than unity. These optical properties indicate the dominance of fine mode pollutant particles over the city. The temperature lapse rate profile within the surface boundary layer has been found to be significantly influenced by the heating effect of fine mode pollutants and, consequently, the growth of the convective processes in the lower troposphere is notably affected. In addition, a back trajectory analysis has also been presented to indicate that transported air masses can have significant impact on spectral pattern of SSA.

**Keywords:** Single scattering albedo, urban pollutants, boundary layer height, temperature lapse rate, convective processes

## 1. Introduction

Aerosol particles, in spite of being a small fraction of atmospheric constituents, influence the Earth's radiation budget significantly by absorbing and scattering solar radiation [Charlson et al., 1992]. Depending on their source and size, the absorption and scattering properties of aerosol drastically vary, which directly affect the aerosol radiative forcing. Aerosol optical depth (AOD) is defined as the extinction of solar irradiance caused by aerosol [Angstrom, 1929] existing within a column of air from ground to the top of the atmosphere. Aerosol single scattering albedo (SSA) is a parameter which contains the information on absorption and scattering properties of aerosol [Haywood and Shine, 1995; Bergstrom and Russell, 1999; Ganguly et al., 2005]. The wavelength dependence of both AOD and SSA provides basic information about the type of aerosols and are commonly used to discriminate the dominance of fine mode and coarse mode particles [Bergstrom et al., 2002; Dubrovik, et al., 2002]. The slope of the logarithm of AOD versus the logarithm of wavelength curve, known as Angström wavelength exponent ( $\alpha$ ), is an indicator of aerosol size [Eck et al, 1999]. A value of  $\alpha$  greater than unity indicate the dominance of fine mode particles associated with urban pollution and a less than unity value indicates dominance of larger aerosol particles like desert dust and sea salts [Bergstrom et al., 2002; Sokolik and Toon, 1997]. For the abundance of urban pollutants, the values of SSA decrease with wavelength whereas for the dust particles dominating over urban pollutants, SSA tends to increase with wavelengths [Bergstrom et al., 2007].

To estimate SSA of aerosol, it is essential to separate the absorption from the total extinction. The absorption due to black carbon (BC) particles is much more dominant compared to any other absorbing particles [Jacobson, 2001; Ramachandran, 2010]. Though BC is a small fraction of total aerosol loading, it can change the aerosol forcing from negative

(cooling) to positive (warming) [Babu et al. 2002; Haywood and Shine, 1997; Heintzenberg et al., 1997]. The importance of BC is considered after CO<sub>2</sub> as a component of global warming [Jacobson, 2001; Bergstrom et al., 2002, Ramanathan and Carmichael, 2008]. BC particles are generated from incomplete combustion of fuels used in vehicles and industries and also from biomass burning [Koelmans et al., 2006; Penner et al., 1993]. Both anthropogenic and natural aerosols play crucial roles to build up the aerosol environment near the land ocean boundary region of Bay of Bengal. Limited studies have been carried out estimating the SSA and Angstrom exponent values over the Gangetic West Bengal region so far [Goto et al., 2011; Lawrence and Lelieveld, 2010]. In our present study the spectral variation of AOD and SSA has been used to classify the dominance of urban pollutant aerosols and dust aerosol particles over Kolkata. Previously, investigators have studied the influence of pollutant aerosols on boundary layer temperature using different models and satellite observations; however the studies are inadequately supported by measurements (Venkatram et al., 1977; Ackerman, 1977; Yoon et. al., 2014). In our study, the impact of pollutant aerosols on boundary layer temperature profile and convective growth has also been investigated over the present location.

## **2. Site and Meteorology**

Kolkata, a metropolitan city in the Eastern part of India, is located near to the land ocean boundary of Bay of Bengal. This is a highly populated city with a heavy traffic load and some industrial belts at the coastal areas of river Ganges. The experimental set up is running at University of Calcutta which is situated in the midst of the city. South-west monsoon is a prevailing meteorological feature experienced in Kolkata when heavy rain fall occurs. It has been reported in articles that nearly 15% of total rainfall over Kolkata takes

place during pre-monsoon (March to May) season [Bhattacharya et al., 2011]. Around 72% of annual rainfall over Gangetic West Bengal as well as over Kolkata, occurs in monsoon (June to September) season [www.imdkolkata.gov.in]. Post-monsoon (October and November) rain is around 10-12% and some occasional rainfall takes place in winter (December to February). Convective rain mostly occurs in pre-monsoon and also in monsoon season. Cloudiness may occur in any season and cloudy sky often hinders aerosol measurement on those days. High humidity and wind from different direction in different time of the year have effects on regional aerosol loading. The boundary layer height over this tropical urban region is maximum in pre-monsoon months and it becomes low in monsoon and winter months..

### **3. Instrument and Data**

Aerosol Optical Depth measurement is carried out at the present location with a multi wavelength radiometer (MWR) with its spectral range from 340nm to 1025nm (ten no. of wavelengths 340, 400, 450, 500, 600, 650, 750, 850, 935, 1025nm). MWR provides the measurements of extinction of directly transmitted solar radiation as a function of solar zenith angle. A 7-channel Aethalometer (AE-31) (Magee Scientific made) is continuously operated at the same location to measure near-surface black carbon concentration at seven wavelengths (370, 470, 520, 590, 660, 880, 950nm). Aethalometer collects ambient air through a cyclone inlet with 5 min interval at a selected constant flow rate of 4 l/min. Seven corresponding wavelengths of MWR (400, 450, 500, 600, 650, 850, 935nm) are used to calculate SSA values. National Center for Environmental Prediction and National Center for Atmospheric Research (NCEP/NCAR) global reanalysis data product of National Oceanic and

Atmospheric Administration (NOAA) (<ftp://arlftp.arlhq.noaa.gov/pub/archives/reanalysis>) has been used in back trajectory analysis. Trajectories are drawn using TrajStat (Trajectory Statistics), which is a geographic information system (GIS) based software. In TrajStat, the trajectory calculation function appears from Hybrid Single Particle Lagrangian Integrated Trajectory (HYSPLIT). HYSPLIT model developed by NOAA's Air Resources Laboratory is one of the most widely used models for atmospheric trajectory and dispersion calculations [Stein et. al., 2015]. Atmospheric boundary layer height (ABLH) data are not measured at the present site. Three hourly gridded data of boundary layer height from 2012-2014 are obtained from NOAA Earth System Research Laboratory (ESRL) data base using the website ([http://www.esrl.noaa.gov/psd/data/gridded/data.20thC\\_ReanV2.monolevel.mm.html](http://www.esrl.noaa.gov/psd/data/gridded/data.20thC_ReanV2.monolevel.mm.html)) and monthly average boundary layer height has been calculated from this data and plotted in Figure 1. Temperature profile data used in this study is measured by a multi-frequency microwave radiometer (RPG-HATPRO) which is continuously operated at this site. The boundary layer temperature lapse rate has been calculated using this temperature profile data. The lapse rate profile averaged over the year shown in Figure 2, has values around 6 K/km and its vertical profile remains almost consistent up to 1km height and above 1 km height lapse rate experiences a notable decrease. For the present study, partially and fully cloudy dates are excluded and only the cloud free days data are taken into account. Cloudiness affects the MWR data set which causes to have limited AOD data for different months. When it is a fully cloudy sky or rainy day MWR is not set to run. The existence of partial cloud coverage over the study location is determined with the help of MWR itself because it gives erroneous reading in the presence of cloud and MWR software itself shows the data set as "Doubtful data". Even if it is found that in case of cloud passing over the region the MWR shows the dataset as "Flat or Zig-Zag" data. So the cloudy dates are easily detectable and are excluded. Only "GOOD data" (for cloud free days) are considered for the study. To have

adequate dataset for each season the data set of 2012 to 2014 has been analyzed. All the data set of AOD, BC and temperature profile used in this study have been collected during the day time [afternoon (AN) (1139 hrs (IST) to 1700 hrs (IST))]of cloud free days.

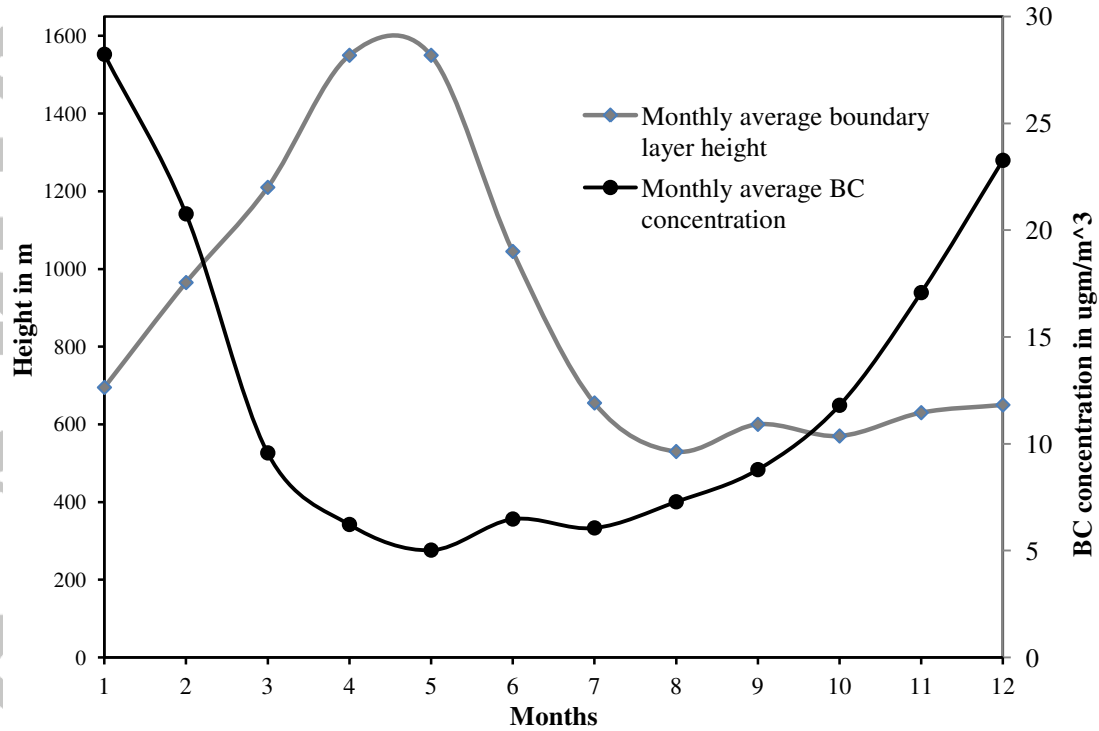


**Figure 1.** Annual variation of Boundary Layer height and near-surface BC concentration over Kolkata

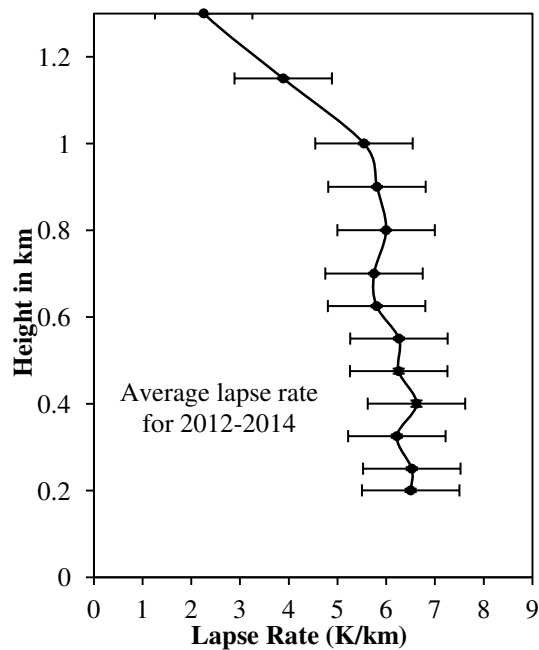


**Figure 2.** Average lapse rate profile (2012-2014) within surface boundary layer (standard deviations of mean are shown by error bars)

#### 4. Methodology

Single scattering albedo ( $\omega$ ) which is the ratio of scattering to the total extinction is calculated by the expression

$$\omega = \frac{\tau_{sca}}{\tau_{sca} + \tau_{abs}} = \frac{\tau_{sca}}{\tau_{\lambda}} \quad (1)$$

Where  $\tau_{abs}$  and  $\tau_{sca}$  are absorption and scattering extinction and  $\tau_{\lambda}$  is AOD. To distinguish two terms  $\tau_{abs}$  and  $\tau_{sca}$ , absorption only due to BC has been taken into account. It has been reported by the earlier researchers that BC is an important constituent (90% of P.M<sub>2.5</sub>) of particulate matter [Tiwari et al., 2013] and second largest heating agents next to CO<sub>2</sub> [Jacobson, 2001; Forster et al., 2007]. A study over Gadanki, India reported that 80 to 90% of net radiation absorbed within the atmosphere is due to soot (Gadhavi and Jayaraman, 2010). It may be noted BC concentration is comparatively much higher over Kolkata than Gadanki. The location of this site being a land-ocean boundary region, the presence of the absorbing aerosols other than BC can be assumed to be negligible [Aruna et. al., 2014]. Absorption coefficient ( $\beta_{abs}$ ) of BC has been calculated using the following equation [Aruna et. al., 2014]

$$\beta_{abs} = \left[ \left( \frac{\Delta ATN}{V} \right) \times A \right] C.R \quad (2)$$

‘C’ and ‘R’ in equation (2) are calibration factors introduced to aethalometer attenuation measurement to have authentic absorption coefficient values. ‘C-factor’ comes due to the multiple scattering of transmitted light by the fibres of the quartz filter [Weingartner et al., 2003] and its value is 1.9 [Bodhaine, 1995]. The second factor ‘R’ is an empirical function incorporated due to the loading of light scattering particles along with BC on the quartz filter and known as ‘shadowing effect’ [Weingartner et al., 2003 and Arnott et al., 2005] and the value of ‘R’ is considered as unity.  $\Delta ATN$  is the change in attenuation of light through filter tape.  $A$  is the spot area of filter tape and  $V$  is the volume of air passed through filter.

The boundary layer height has a profound control on near-surface BC concentration. It has also been reported in earlier studies that most of the BC particles are contained within the atmospheric boundary layer height and are mixed homogeneously [Stull, 1988; Gogoi et al., 2011; Aruna et al., 2014]. Figure 1 shows that the average boundary layer height over this tropical urban region in pre-monsoon months is around 1.5 km, in monsoon it decreases up to around 600 m and in winter months it is around 760m. Such differences in boundary layer height during rainy and winter season in comparison with the summer or pre-monsoon season are in good agreement with the findings by Guo et al. (2016). Figure 1 also shows that monthly mean BC concentration near to the surface drastically decreases when boundary layer height increases. It has been considered by earlier researchers in their studies that major fraction of BC particles is contained within ABL height. Though, BC is practically present there above ABL height [Babu et al., 2011]. In the present study, we have considered the existence of BC only within the boundary layer height for the simplification of calculations. The presented values of absorption due to BC, in this paper are somewhat underestimated. If the contribution of BC present above ABL would be taken into the account the absorption due to BC would be found higher than the present values and the consequences would be more prominent than the present one. This however, does not change the overall propositions of the study.

Under these conditions, extinction due to BC ( $\tau_{abs}$ ) has been calculated by multiplying the atmospheric boundary layer height [Aruna et al., 2014] (ABLH data used is not retrieved, it is NOAA ESRL gridded data) with the derived value of absorption coefficient ( $\beta_{abs}$ ) of BC.

$$\tau_{abs} = ABLH \times \beta_{abs} \quad (3)$$

The scattering extinction ( $\tau_{sca}$ ) is calculated by subtracting the  $\tau_{abs}$  values from  $\tau_{\lambda}$  for different wavelengths as available.

$$\tau_{sca} = \tau_{\lambda} - \tau_{abs} \quad (4)$$

and SSA has been derived by using equation (1).

The spectral dependence of AOD is used to calculate the Angström exponent ( $\alpha$ ).

AOD is related to Angström exponent by the equation

$$AOD_{\lambda} = \beta \lambda^{-\alpha} \quad (5)$$

Angström exponent ( $\alpha$ ) is an indicator of the particle size. Using linear regression in the equation,

$$\ln AOD_{\lambda} = -\alpha \ln \lambda + \ln \beta \quad (6)$$

$\alpha$  is determined by the slope of the line.  $\beta$  is atmospheric turbidity coefficient.

## 5. Results and discussions

### 5.1. Seasonal variation of AOD and SSA

Average AOD (500nm) over Kolkata is high (~1) in winter and comparatively lower (0.6 to 0.7) in monsoon and post-monsoon months with a yearly average of 0.8 as shown in Figure 3(a). Average AOD value of a monsoon month, June has not been presented here due to paucity of data during this month. The spectral variation of AOD is shown in Figure 3(b). It depicts a definite decreasing pattern with wavelength in every season and this spectral variation does not show significant seasonal change over the year. Figure 3(c) shows that the absorption coefficient of black carbon aerosol has higher values (~.0002) in winter months compared to the other months and Figure 3(d) shows that absorption coefficient decreases with wavelengths in every season. It is shown in Figure 3(e) that monthly average SSA values vary between ~0.78 to ~0.96 with a yearly average of 0.87 and maximum value in

monsoon season. It is noted that SSA values are lowest in pre-monsoon and absorption coefficient values are also low in this season. Apparently, it may appear inconsistent but boundary layer plays a significant role here. In pre-monsoon season, the atmospheric boundary layer height drastically increases. This causes a well mixing of absorbing particles throughout the extended boundary layer which results in the dilution of near surface concentration of absorbing particles. However, the net absorption due to the extended layer of absorption particles does not decrease indeed. The spectral variation of SSA is shown in Figure 3(f) indicating that SSA decreases with the wavelength except in the monsoon season.

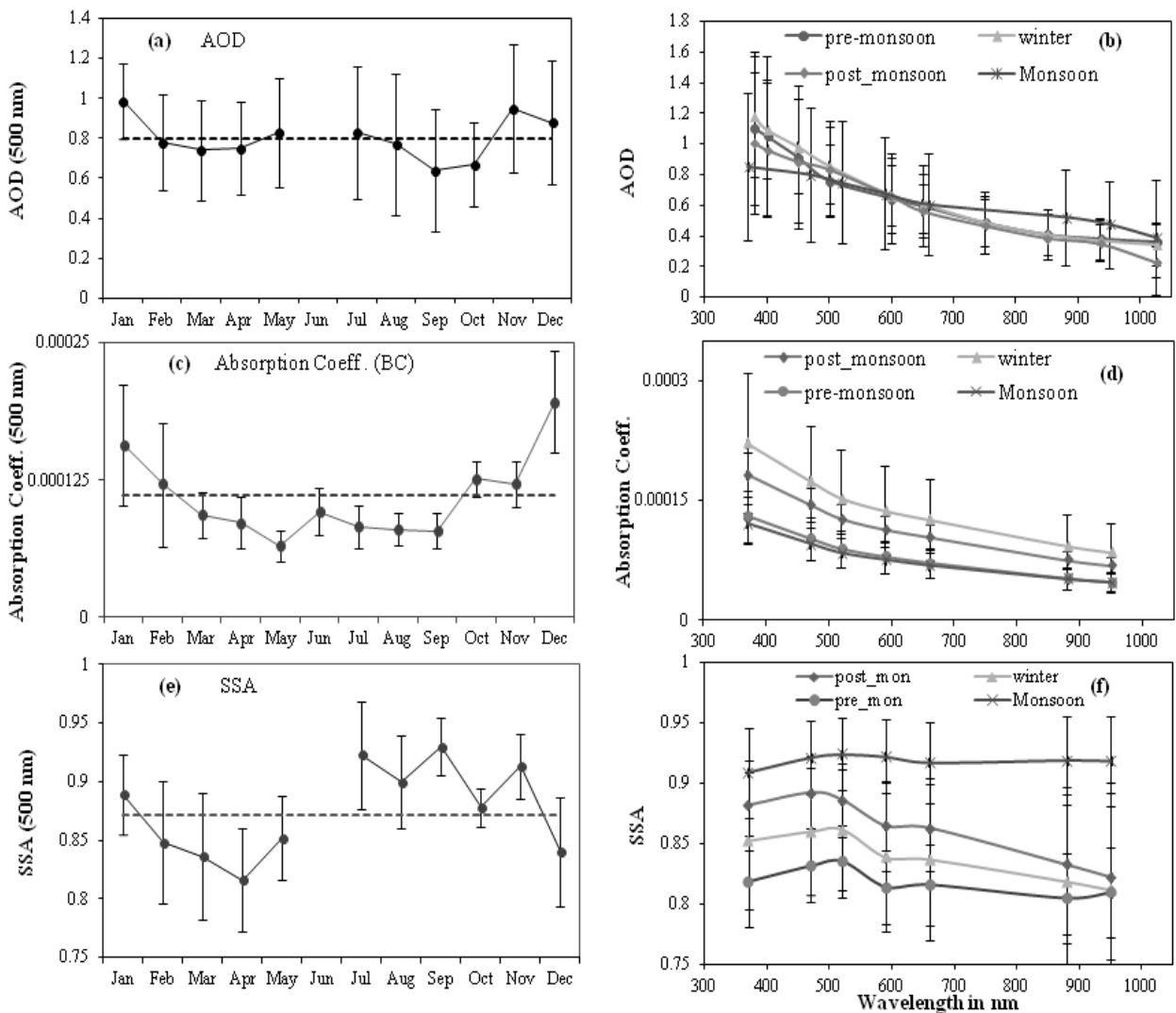


**Figure 3.** Annual variation of (a) AOD (c) absorption coefficient and (e) SSA at 500 nm. Seasonal variation of the spectral patterns of (b) AOD, (d) absorption coefficient and (f) SSA (standard deviations of monthly mean are shown by error bars)

The spectral pattern of SSA observed in post-monsoon, winter and pre-monsoon season reflects the dominance of fine mode pollutant particles at the present location.

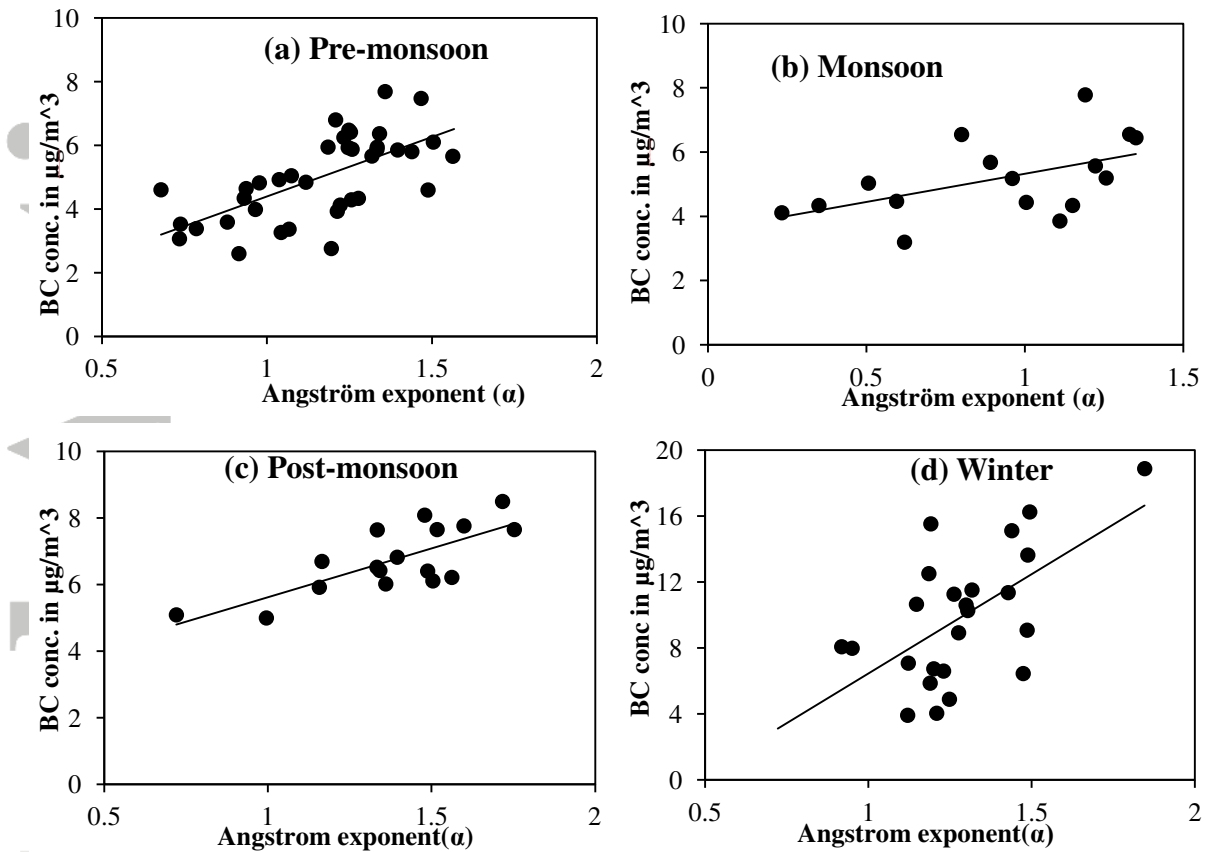


**Figure 4.** Correlations between near-surface BC concentrations and Angström exponent ( $\alpha$ ) values in (a) pre-monsoon, (b) monsoon, (c) post-monsoon and (d) winter of 2012-13

BC particle because of its high absorption efficiency plays an important role in determining the spectral tendency of SSA [Bergstrom et al., AMS, 2002]. In this highly populated urban region, significant amounts of BC are present in its environment because of their continuous generation from vehicular emission [Talukdar et al., 2015]. It has been observed that BC shows positive correlation of its concentration with  $\alpha$  in every season as depicted in Figure 4. This also reveals the significance of BC near-surface concentration in total aerosol loading over this urban region.

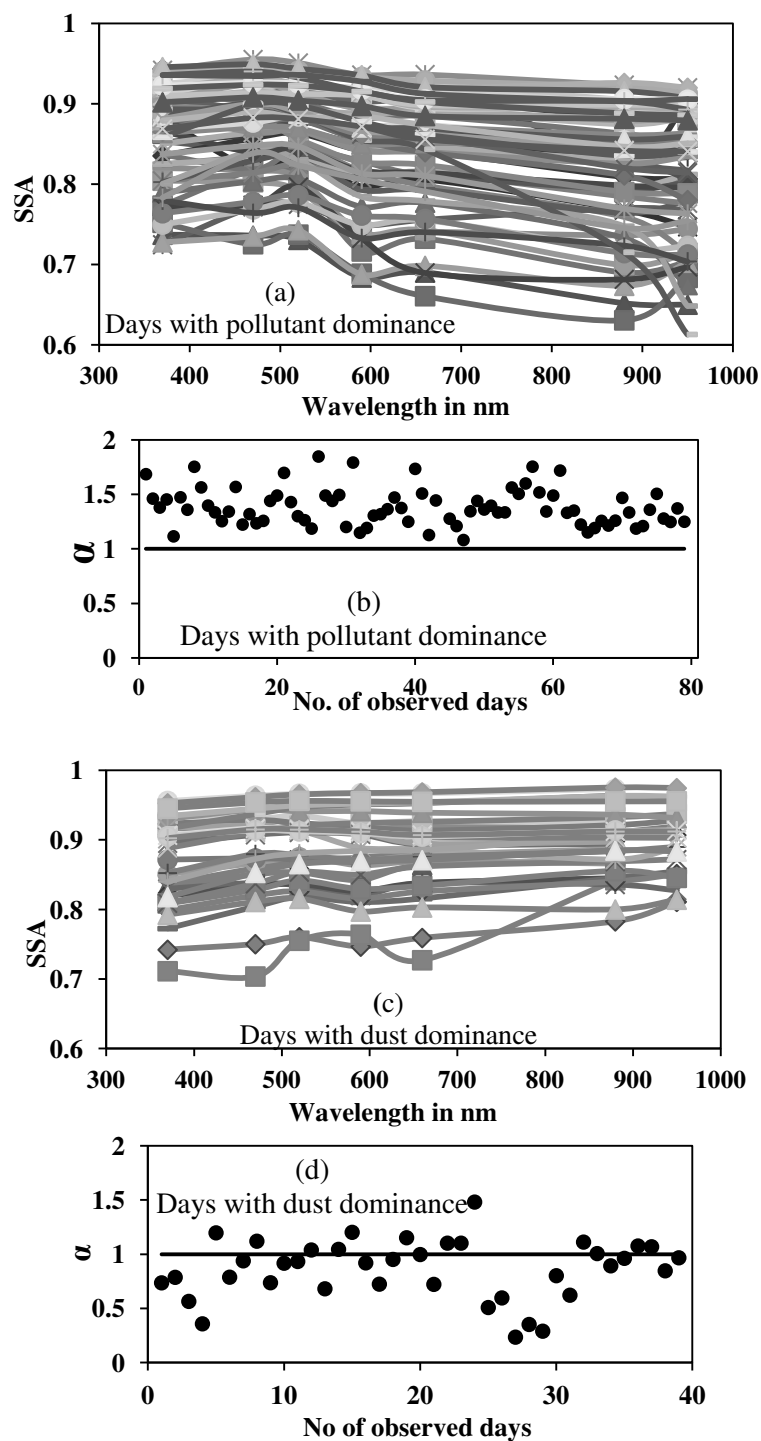


**Figure 5.** Wavelength dependence of SSA (a) decreasing with wavelengths and (b) corresponding Angstrom exponent values (c) SSA increasing with wavelengths and (d) corresponding Angstrom exponent values

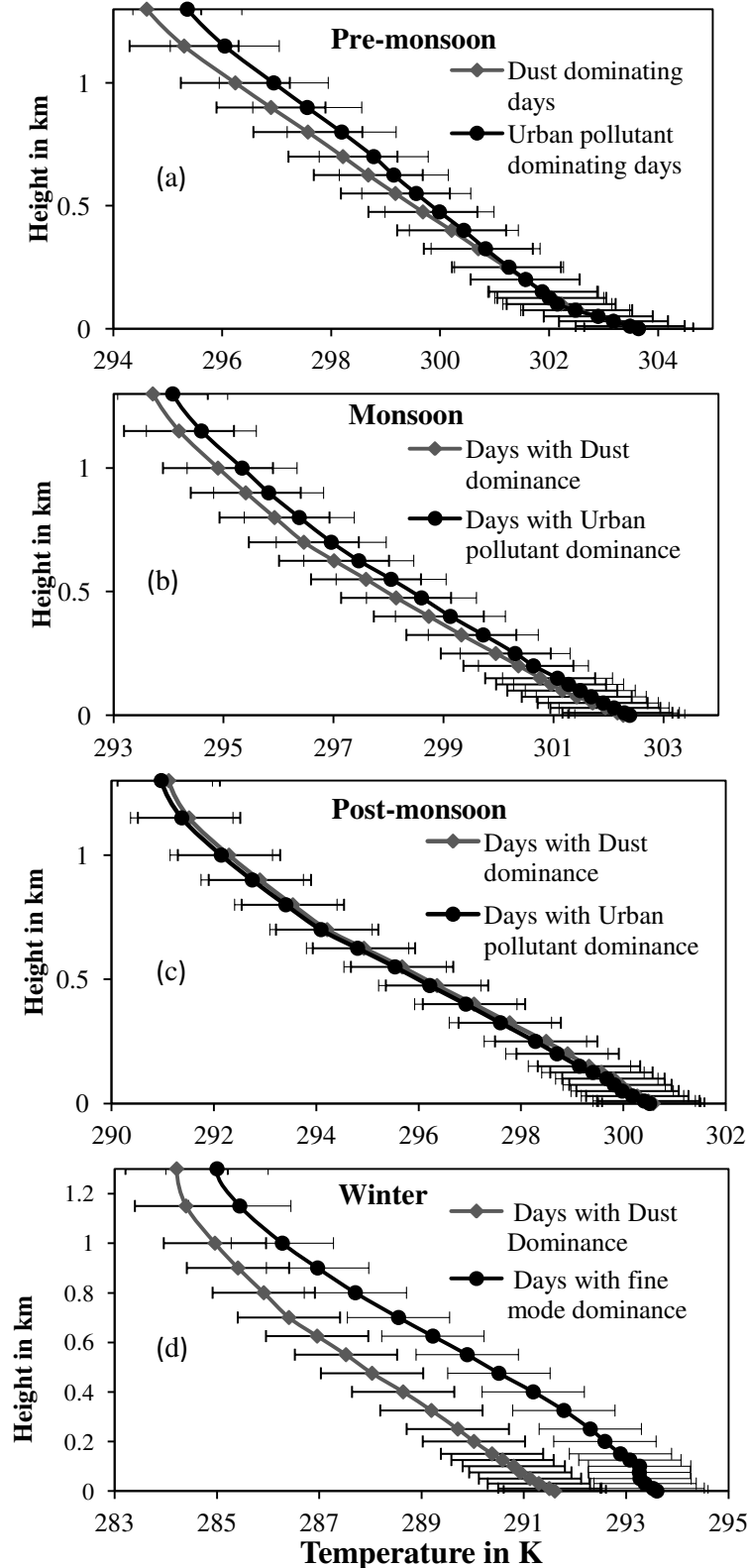
Though the spectral variation of SSA mostly shows decreasing trend and corresponding  $\alpha$  are found to have values greater than unity as shown in Figure 5(a) and 5(b) indicating the dominance of fine mode pollutants, it is observed in Figure 5(c) and 5(d) that

on a number of days the spectral variation of SSA shows an increasing trend and  $\alpha$  calculated for most of those days is less than unity which indicates the dominance of dust mode aerosols on those days.

## 5.2. Impact of pollutant particles on boundary layer temperature profile

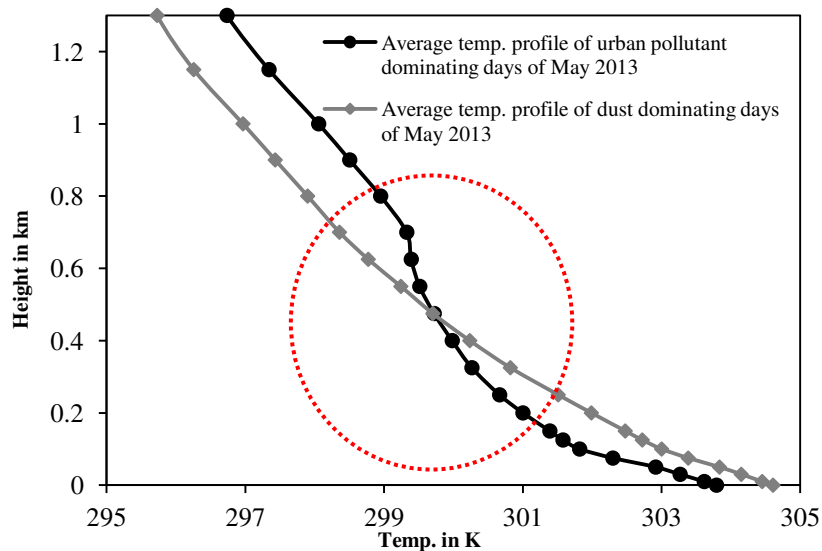
Urban pollutants are considered to be dominated by light absorbing carbon (LAC) which is highly absorbing in nature (Bergstrom et. al 2007) and effectively take part in warming up of the atmosphere. The impact of the abundance of pollutant particles on local temperature profile has been investigated in the present study. We have examined the temperature profile within the boundary layer for the group of days having pollutant particle dominance and separately for the group of days which have dust particle dominance in different seasons. It has been observed from the temperature profile as shown in Figure 6, that pollutant dominating days have comparatively higher temperature than that of the dust dominating days. The difference is most prominent during winter. It has been mentioned in the previous section that the absorption coefficient value is maximum in winter and it is also reported in earlier studies that BC particles have their maximum concentration near the ground during winter [Talukdar et al., 2015] when boundary layer height is low with an average value around 760 m (average value during December: 655.7 m, January: 701.9 m, February: 952.1 m) at this present location. Similar observations of boundary layer height during winter month have been also reported in an early study by Niranjana et al., (2006) over the Indo-Gangetic plain. These suggest that the shallowness of boundary layer along with the presence of temperature inversion in winter causes a rapid increase in the concentration of pollutant particles near to the surface which warms the bottom level of the boundary layer resulting in a significant increase in near surface temperature profile. Aerosols could be further amplified by the feedback between aerosol and PBL or between aerosol and surface

wind (Yang et al. 2016) The above mentioned difference in temperature profile is not prominent in monsoon and post-monsoon which may be due to the wet removal of absorbing aerosols from the atmosphere [Kohler et al., 2001; Dumaka et. al., 2010].

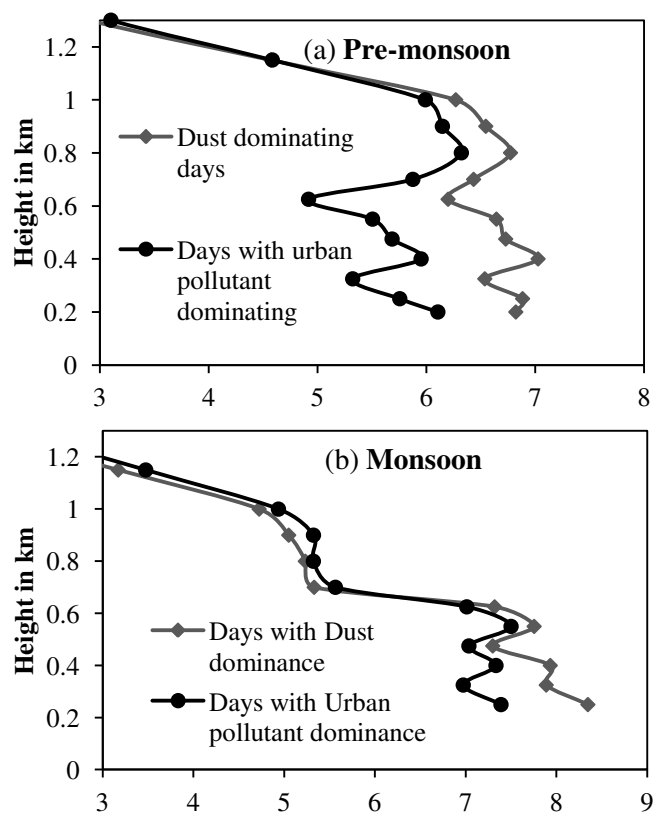


**Figure 6.** Near surface temperature profiles compared on dust dominating days and urban pollutant dominating days in (a) pre-monsoon (b) monsoon (c) post-monsoon and (d) winter (standard deviations of mean value are marked by error bars)

However, in pre-monsoon months also a notable difference in temperature profile among the mentioned two group of days has been noticed. The extended boundary layer height in the pre-monsoon season allows a homogeneous mixing of pollutant particles within this layer [Tiwari et al., 2013; Saha et al., 2014] and absorbs much solar radiation throughout this extended height. This may cause a significant decrease in lapse rate within the boundary layer on pollutant dominating days compared to the dust dominating days in the pre-monsoon season. Figure 7 compares the temperature profiles of pollutant dominating days with dust dominating days during a pre-monsoon month (May 2013). It is distinctively observed from the Figure that the vertical gradient of temperature in the height range 200 m to 800 m on pollutant dominating days is notably different compared to that of the dust dominating days. The mentioned change in temperature profile will result in a sharp decrease in lapse rate profile on pollutant dominating days. To observe the decrease more evidently, the lapse rate within the boundary layer for pollutant dominating days are compared with dust dominating days in each of the four seasons separately. Figure 8 shows that the temperature lapse rate within the boundary layer has a noteworthy decrease in pre-monsoon season for the pollutant dominating days compared to the dust dominating days. In other seasons this difference becomes insignificant.



**Figure 7.** Comparison between the vertical gradient of average temperature profiles (marked portion of the plot) on pollutant dominating days and dust dominating days (May 2013)



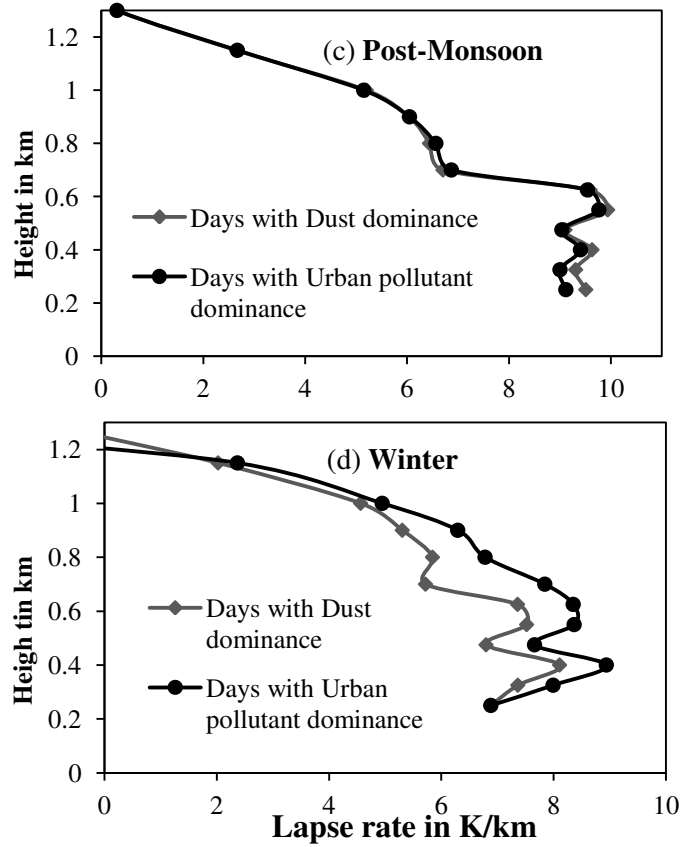


**Figure 8.** Boundary layer temperature lapse rate of dust dominating days and pollutant dominating days in (a) pre-monsoon, (b) monsoon, (c) post-monsoon and (d) winter

### 5.3. Effect of pollutant particles on temperature lapse rate and convective processes

Temperature lapse rate strongly influences the growth of convective processes. Convective available potential energy (CAPE) is a useful instability index to measure the development of convective process [Holton, 2004]. In our further study the decrease in lapse rate on pollutant dominating days and the corresponding CAPE values for those days during pre-monsoon season has been intensively examined. The mathematical equation of CAPE is expressed as

$$CAPE = \int_{Z_{LFC}}^{Z_{LNB}} g \left( \frac{T_{parcel} - T_{env}}{T_{env}} \right) dz \quad (7)$$

Here  $T_{parcel}$  and  $T_{env}$  are designated for moist air parcel temperature and temperature of the environment respectively. The lower and upper limit of the integration is level of free convection  $Z_{LFC}$  and the level of neutral buoyancy  $Z_{LNB}$ . The equation (7) indicates that a small change in the temperature lapse rate profile will significantly affects the value of CAPE. We have intended to observe the probable impact of abundance of pollutant particles on the growth of convective energy over the present location during pre-monsoon season when the convective processes are likely to occur. A window of 10 day time span during pre-monsoon have been considered and within this span of time, pollutant dominating days and dust dominating days are grouped separately. The lapse rate profiles for the group of urban pollutant dominating days are compared with the group of dust particle dominating days. This window of 10 day time span has been taken to avoid or minimize the effect of temporal variability in temperature profile as well as in the lapse rate. The difference in lapse rate due to pollutants will be effectively more notable through this observation avoiding the change in temperature and lapse rate due to seasonal or temporal variations. Some of the comparisons of lapse rate profiles shown in Figure 9 depict that the lapse rate of pollutant dominating days are prominently less than that of the dust dominating days in pre-monsoon.

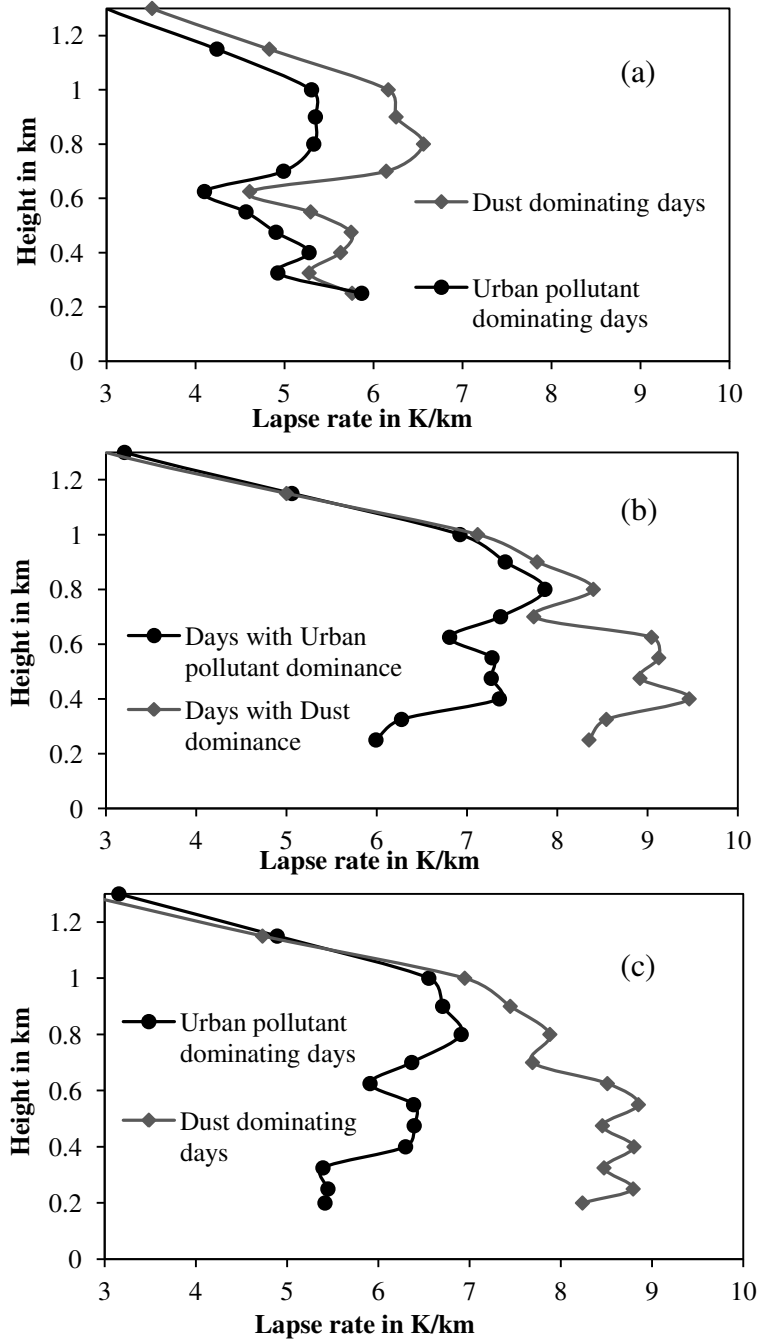


**Figure 9.** Boundary layer temperature lapse rate for different groups of pollutant dominating days and dust dominating days during pre-monsoon season. Three sets of example each group with 10 days time span, are presented: (a) 24 April – 3 May, 2012 (b) 15 March- 24March, 2013 and (c) 25 March- 3 April, 2014

This prominent decrease in lapse rate associated with the pollutant dominating days may cause to reduce the convection of wind and thus the growth of the convective processes within boundary layer may be affected [Parameswaran et al., 2004; Niranjana et al., 2006]. The delayed growth could be due to the effect of aerosol-radiation interaction (ARI),

accompanied by the effect of aerosol-cloud interaction (ACI) (Guo et al., 2016; Lee et al., 2016). It has been observed from our investigations that day time CAPE values are much lower on the days which experience dominance of urban pollutants compared to the days having dominance of dust aerosols. Figure 10 shows an example of the mentioned fact that the day time maximum CAPE values are comparatively lower on a pollutant dominating day than a dust dominating day.

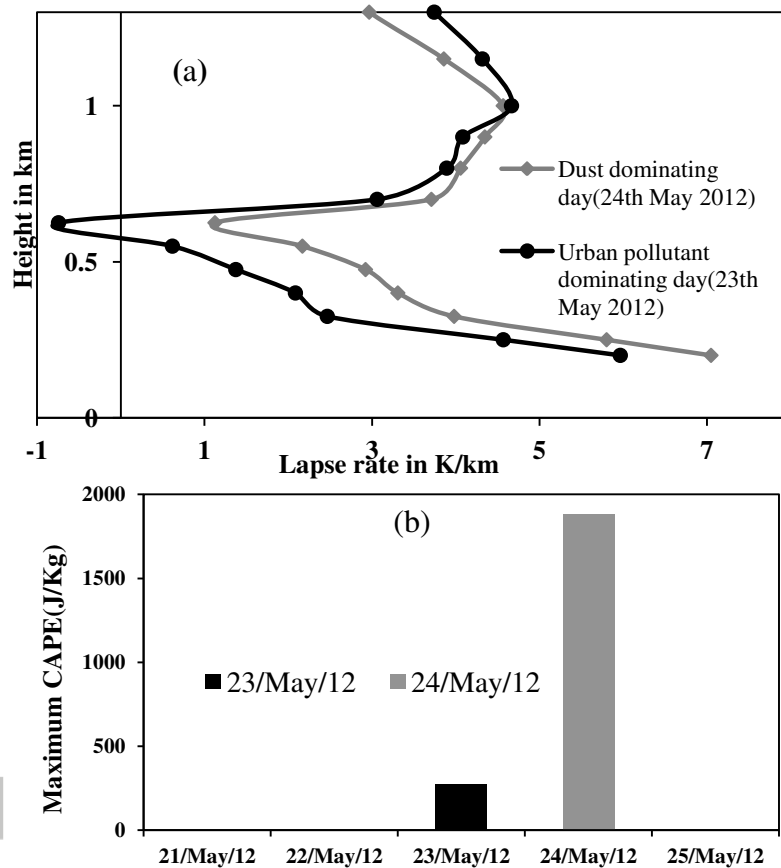


**Figure 10.** Comparison between (a) lapse rate for a pollutant dominating day (23 May 2012) and dust dominating day (24 May 2012) and (b) corresponding CAPE values

Figure 10 (a) shows the temperature lapse rate profile of a pollutant dominating day (23 May 2012) has a negative value at around 600 meter height which indicates the presence of temperature inversion at that height. Temperature inversion directly affects the normal convection in the atmosphere which has caused to reduce the maximum CAPE value (359 J/Kg) on that day. Whereas on the consequent day (24 May 2012) which is a dust dominating

day and the lapse rate is comparatively higher than the previous day, it has been found that the maximum CAPE value (1870 J/Kg) is around 5times higher than the pollutant dominating day.

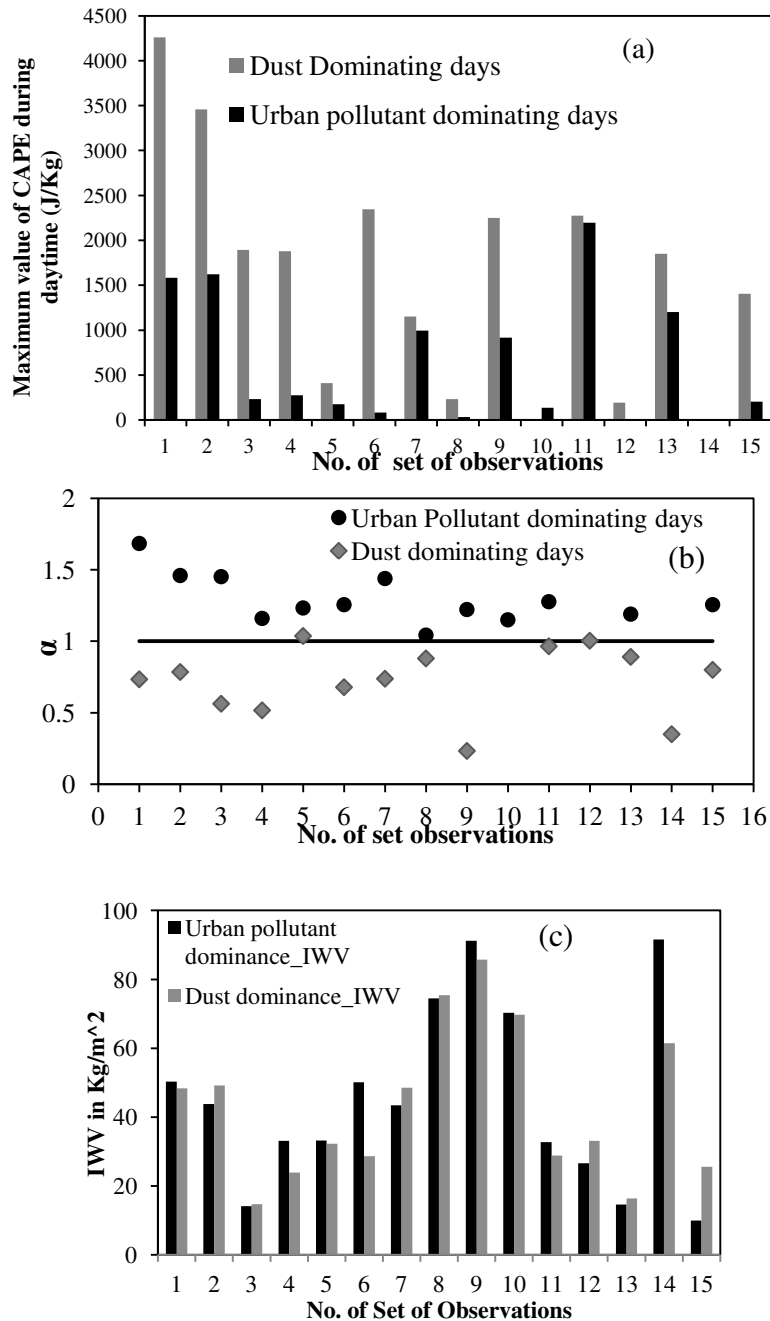


**Figure 11.** (a) Maximum CAPE values compared between dust dominating days and pollutant dominating days, (b) Angstrom Exponent values for corresponding days (c) Corresponding IWV values

This very decrease in lapse rate associated with the abundance of urban pollutants may affect the convective activities in pre-monsoon season over the urban locations like the present one. It has been found that the maximum CAPE values during day time on pollutant dominating days have lower values compared to the dust dominating days in most of the observed cases during pre-monsoon season as shown in Figure 11(a). To examine whether integrated water vapour (IWV) contributed significantly to the change in CAPE values in these two cases, we compared the IWV amount (using our radiometric observation data) for dust dominating days and pollutant dominating days. Figure 11(c) shows that there is no notable difference in IWV values between these two cases which substantiate the fact that the decrease in lapse rate in association with the dominance of pollutant aerosols mostly influenced the weakening of convective processes.

#### 5.4. Role of transported air mass

In the present study we have also analyzed the back trajectories for all the dates under our observation. A 5-day back trajectory has been presented using TrajStat for all the dust dominating days and pollutant dominating days separately. From the analysis it has been observed that the trajectories (at 2000 m agl) for pollutant dominating days are arriving from Indian sub-continental region whereas, trajectories for dust dominating days are found to travel mostly from the arid region of Middle-East as shown in the Figure 12 (a), (b). This feature is not prominent if the trajectories are drawn for 1000 m above ground level (agl) which can be due to the turbulences present within this height of the boundary layer [Garratt, 1992]. It has been also reported by earlier researchers that only the higher trajectories are capable of long-range transport [Gogoi et al., 2009]. The transported air mass at 2000 m agl from the arid region of Middle-east may carry dust aerosols which may alter the dominance

of locally generated aerosols into the dominance of dust particles. On the other hand the air mass transported from the land part of the Indian subcontinent will have the probability of carrying anthropogenic aerosols which can increase the regional concentration of fine mode particles. It points to the fact that transported air mass has strong association with regional aerosol loading which can influence the wavelength dependence pattern of SSA.

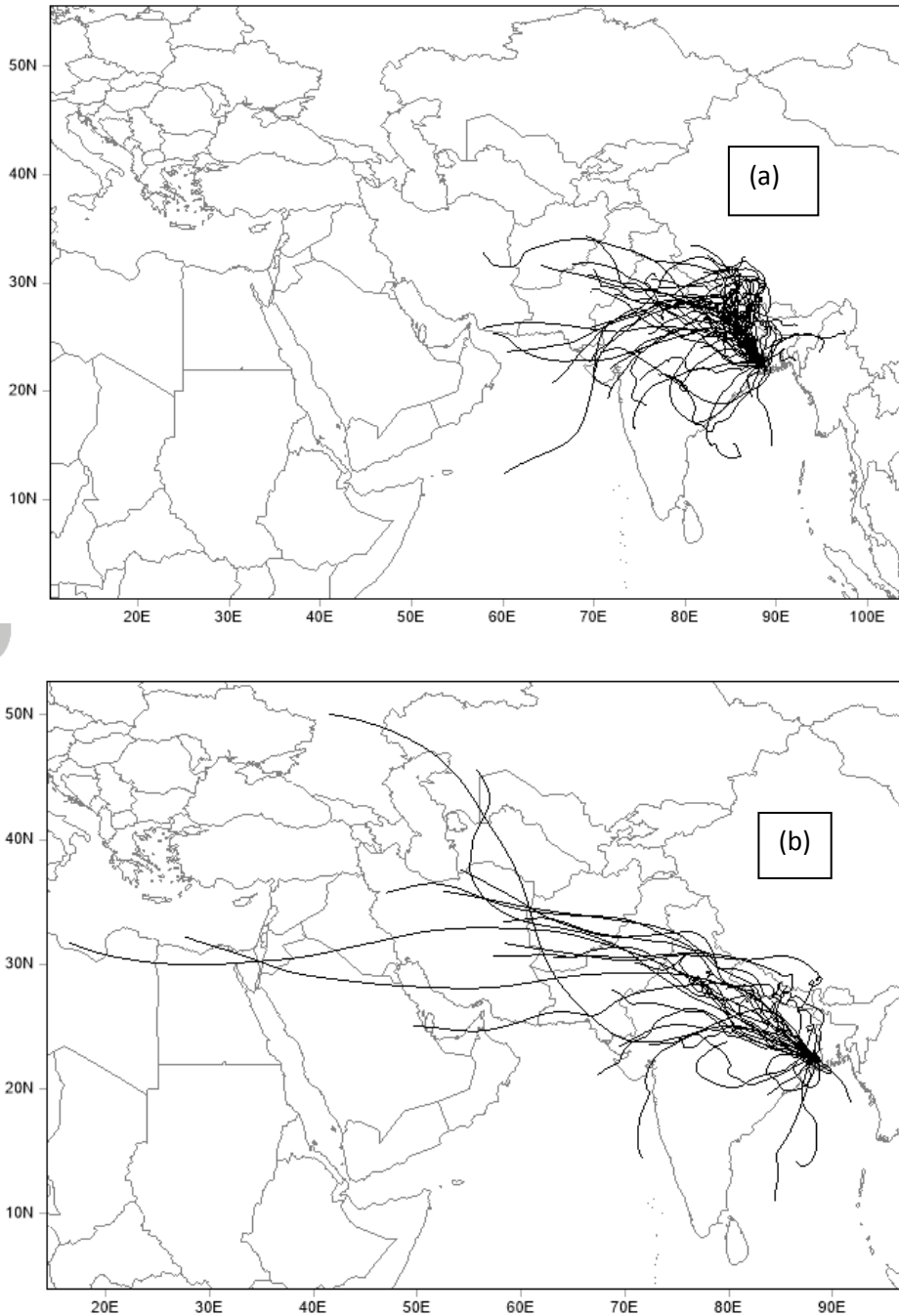


**Figure 12.** Back Trajectories (at 2000 m agl) for (a) urban pollutant dominating days and (b) dust dominating days

In monsoon the wavelength dependence of SSA mostly shows an increasing trend with wavelength indicating a less dominance of fine mode particles during this season. Unlike the other seasons it has been observed in monsoon that back trajectories are not arriving from far distances even on those days when  $\alpha$  value is less than unity and SSA increases with wavelengths. The scavenging of aerosols due to rain fall in monsoon and the presence of marine aerosol in south westerly air mass may have a stronger control on the total aerosol loading at this location [Moorthy et al., 1997]. Comparatively larger size of marine aerosol may cause to change spectral pattern of SSA in monsoon season.

## 6. Summary

This paper presents the results on the observations of the aerosol optical properties over Kolkata primarily utilizing the ground based measurements. The observations from such a region, which is a densely populated urban location near to the land-ocean boundary in Eastern India, are inadequately available in open literature so far. The main conclusions of our study are as follows:

[1] The present study discriminates the dominance of urban pollutant aerosols and dust aerosols over Kolkata using the spectral dependence of AOD and SSA during different seasons of a year. The spectral dependence of aerosol optical depth and single scattering albedo points to the dominance of fine mode pollutant aerosols for most of the time in a year over the present urban region. This is also supported by the fact that the corresponding Angstrom coefficient values become greater than unity.

[2] Aerosol optical depths over Kolkata are high ( $\sim 1$ ) in winter and comparatively low (0.6 to 0.7) in monsoon and post-monsoon months with a yearly average of 0.8.

[3] Single scattering albedo is minimum in pre-monsoon months with average values of 0.8 to 0.85 and maximum in monsoon months with average values of 0.9 to 0.95. In monsoon the spectral dependence of SSA does not show decreasing trend, unlike the other seasons, indicating a lower concentration of fine mode pollutants in this season.

[4] The abundance of pollutant aerosols in this urban environment affects the temperature lapse rate within the boundary layer. It is particularly observed that the vertical gradient of temperature within the boundary layer height on pollutant dominating days is notably different compared to that on the dust dominating days, especially in pre-monsoon months hindering the growth of convective processes during this season.

[5] In the winter, a notable increase in boundary layer temperature has been observed in association with the dominance of pollutant aerosols in this region.

[6] Back trajectory analysis indicates to the possibility of the transport of anthropogenic aerosols from the land part of the Indian subcontinent which additionally contributes to the regional concentration of fine mode particles.

[7] The air mass transported from the arid region of the Middle-east carry dust aerosol particles (desert dust) which influence the spectral pattern of SSA at the present location.

### **Acknowledgments**

This work has been supported by the grants from the Indian Space Research Organization under the Project “Studies on Aerosol Environment at Kolkata Located Near the Land-Ocean Boundary as a Part of ARFI Network under ISRO-GBP” being carried out at S.K. Mitra Centre for Research in Space Environment, University of Calcutta. National Center for Environmental Prediction and National Center for Atmospheric Research (NCEP/NCAR) global reanalysis data product of National Oceanic and Atmospheric Administration (NOAA)

(<ftp://arlftp.arlhq.noaa.gov/pub/archives/reanalysis>) has been used in back trajectory analysis

Atmospheric boundary layer height data are obtained from NOAA Earth System Research Laboratory (ESRL) data base using the website

([http://www.esrl.noaa.gov/psd/data/gridded/data.20thC\\_ReanV2.monolevel.mm.html](http://www.esrl.noaa.gov/psd/data/gridded/data.20thC_ReanV2.monolevel.mm.html))

## References

Angstrom, A., (1929), On the atmospheric transmission of Sun radiation and on dust in the air, *Geogr. Ann.*, 11, 156– 166.

Arnott, W.P., K. Hamasha, H. Moosmuller, P.J. Sheridan, and J.A. Ogren, (2005), Towards aerosol light absorption measurements with a 7-wavelength aethalometer: evaluation with a photoacoustic instrument and 3-wavelength nephelometer, *Aerosol Science and Technology*, 39, 17–29.

Aruna K., T.V. LakshmiKumar, D. NarayanaRao, B. V. KrishnaMurthy, S. S. Babu, and K. Krishnamoorthy, (2014), Scattering and absorption characteristics of atmospheric aerosols over a semi-urban coastal environment, *Journal of Atmospheric and Solar-Terrestrial Physics*, 119, 211–222.

Babu, S. S., S. K. Satheesh, and K. K. Moorthy, (2002), Aerosol radiative forcing due to enhanced black carbon at an urban site in India, *Geophys. Res. Lett.*, 29(18), 1880, doi:10.1029/2002GL015826.

Babu, S. S., K. K. Moorthy, R. K. Manchanda, P. R. Sinha, S. K. Satheesh, D. P. Vajja, S. Srinivasan, and V. H. A. Kumar (2011), Free tropospheric black carbon aerosol measurements using high altitude balloon: Do BC layers build “their own homes” up in the atmosphere?, *Geophys. Res. Lett.*, 38, L08803, doi:10.1029/2011GL046654.

Bergstrom, R. W., and P. B. Russell, (1999), Estimation of aerosol direct radiative effects over the mid-latitude North Atlantic from satellite and in situ measurements, *Geophys. Res. Lett.*, 26, 1731–1734.

Bergstrom, R. W., P. B. Russell, and P. Hignett, (2002), Wavelength Dependence of the Absorption of Black Carbon Particles: Predictions and Results from the TARFOX Experiment and Implications for, *J. Atmos. Sci.*, 59, 567-577.

Bergstrom, R. W., P. Pilewskie, P. B. Russell, J. Redemann, T. C. Bond, P. K. Quinn, and B. Sierau, (2007), Spectral absorption properties of atmospheric aerosols, *Atmos. Chem. Phys.*, 7, 5937–5943.

Bodhaine, B.A., (1995), Aerosol absorption measurements at Barrow, Mauna Loa and the South Pole. *J. Geophys. Res.*, 100, 8967–8975.

Bhattacharya, R., A. Bhattacharya, R. Das, S. Pal and P. Mali, (2011), Premonsoon climate and rainfall activity over West Bengal: A survey, *International J. Phys*, 4, 141-148.

Charlson, R.J., S.E. Schwartz, J.M. Hales, R.D. Cess, J.A. Coakley, J.E. Hansen, and D.J. Hofmann, (1992), Climate forcing by anthropogenic aerosols, *Science*, 255, 423–430.

Dubovik, O., B. N. Holben, T. F. Eck, A. Smirnov, Y. J. Kaufman, M. D. King, D. Tanre, and I. Slutsker, (2002), Climatology of atmospheric aerosol absorption and optical properties in key locations, *J. Atmos. Sci.*, 59, 590–608.

Dumka, U.C., and K. Krishna Moorthy, (2010), Characteristics of aerosol black carbon mass concentration over a high altitude location in the Central Himalayas from multi-year measurements, *Atmos. Res.*, 96, 510–521.

Eck, T. F., B. N. Holben, J. S. Reid, O. Dubovik, A. Smirnov, N. T. O'Neill, I. Slutsker, and S. Kinne, (1999), Wavelength dependence of the optical depth of biomass burning, urban, and desert dust aerosols, *J. Geophys. Res.*, 104, 31,333–31,349.

Gadhavi, H., and Jayaraman, A., Absorbing aerosols: contribution of biomass burning and implications for radiative forcing, *Ann. Geophys.*, 28, 103–111.

Ganguly, D., H. Gadhavi, A. Jayaraman, T. A. Rajesh, and A. Misra, (2005), Single scattering albedo of aerosols over the central India: Implications for the regional aerosol radiative forcing, *Geophys. Res. Lett.*, 32, L18803, doi:10.1029/2005GL023903.

Garratt, J. R., 1992. *The atmospheric boundary layer*. Cambridge University Press, P. 168.

Gogoi, M. M., K. K. Moorthy, S. S. Babu, and P. K. Bhuyan, (2009), Climatology of columnar aerosol properties and the influence of synoptic conditions: First-time results from the northeastern region of India, *J. Geophys. Res.*, 114, D08202, doi:10.1029/2008JD010765.

Gogoi, M. M., Pathak, B., Moorthy, K. K., Bhuyan, P. K., Babu, S. S., Bhuyan, K. and Kalita, G. (2011). Multi-year Investigations of near Surface and Columnar Aerosols over Dibrugarh, Northeastern Location of India: Heterogeneity in Source Impacts. *Atmos. Environ.* 45: 1714–1724.

Goto, D., T. Takemura, T. Nakajima, and K.V.S. Badarinath, (2011), Global aerosol model-derived black carbon concentration and single scattering albedo over Indian region and its comparison with ground observations, *Atmos. Environ.* 45, 3277–3285.

Guo, J., Miao, Y., Zhang, Y., Liu, H., Li, Z., Zhang, W., He, J., Lou, M., Yan, Y., Bian, L., and Zhai, P.(2016), The climatology of planetary boundary layer height in China derived from radiosonde and reanalysis data, *Atmos. Chem. Phys.* 16, 13309-13319., doi:10.5194/acp-16-13309-2016

Guo, J., M. Deng, S. S. Lee, F. Wang, Z. Li, P. Zhai, H. Liu, W. Lv, W. Yao, and X. Li (2016), Delaying precipitation and lightning by air pollution over the Pearl River Delta. Part I: Observational analyses, *J. Geophys. Res. Atmos.*, 121, 6472-6488, doi:10.1002/2015JD023257.

Haywood, J. M., and K. P. Shine, (1995), The effect of anthropogenic sulphate and soot aerosols on clear sky planetary radiation budget, *Geophys. Res. Lett.*, 22, 603–605.

Haywood, J. M., and K. P. Shine, (1997), Multi-spectral calculations of the radiative forcing of tropospheric sulphate and soot aerosols using a column model, *Q. J. R. Meteorol. Soc.*, 123, 1907– 1930.

Heintzenberg, J. R., R. J. Charlson, A. D. Clarke, C. Liousse, V. Ramaswamy, K. P. Shine, and M. Wendisch, (1997), Measurement and modelling of aerosol single scattering albedo: Progress, problems and prospects, *Contrib. Atmos. Phys.*, 70, 249–264.

Holton, J. R., (2004), *An Introduction to Dynamic Meteorology*. (Fourth Edition) Elsevier Academic Press, California, USA.

Jacobson, M.Z., (2001), Strong radiative heating due to the mixing state of black carbon on atmospheric aerosols, *Nature*, 409, 695–697.

Koelmans, A.A., M. T.O. Jonker, G. Cornelissen, T. D. Bucheli, Paul C.M Van Noort, and Ö. Gustafsson, (2006), Black carbon: the reverse of its dark side, *Chemosphere*, 63, 365–377.

Kohler, I., M. Dameris, I. Ackermann, and H. Hass, (2001), Contribution of road traffic emissions to the atmospheric black carbon burden in the mid-1990s, *J. Geophys. Res.*, 106(No.D16), 17997–18014.

Lawrence, M.G., and J. Lelieveld, (2010), Atmospheric pollutant outflow from southern Asia: a review, *Atmos. Chem. Phys.*, 10, 11017e11096.

Lee, S.-S., Guo, J.P., Z. Li, 2016. Delaying precipitation by air pollution over Pearl River Delta. Part 2: model simulations, *J. Geophys. Res.:Atmos.*, 121, 11,739-11,760, doi:10.1002/2015JD024362.

Moorthy, K. K., S. K. Satheesh, B. V. K. Murthy, (1997), Investigations of marine aerosols over the tropical Indian Ocean, *J. Geophys. Res.*, 102, 18827–18842, 1997.

Niranjan, K., V. Sreekanth, B. L. Madhavan, and K. Krishna Moorthy (2006), Wintertime aerosol characteristics at a north Indian site Kharagpur in the Indo-Gangetic plains located at the outflow region into Bay of Bengal, *J. Geophys. Res.*, 111, D24209, doi:10.1029/2006JD007635.

Parameswaran, K., S. V. Sunilkumar, K. Rajeev, P. R. Nair, and K. Krishna Moorthy (2004), Boundary layer aerosols at Trivandrum tropical coast, *Adv. Space Res.*, 34, 838–844.

Penner, J.E., H. Eddleman, and T. Novakov, (1993), Towards the development of a global inventory for black carbon emissions, *Atmos. Environ.*, 27, 1277–1295.

Ramachandran S., and S. Kedia, (2010), Black carbon aerosols over an urban region: Radiative forcing and climate impact, *J. Geophys. Res.*, 115, d10202, doi:10.1029/2009jd013560,

Ramanathan, V., and G. Carmichael, (2008), Global and regional climate changes due to black carbon, *Nat. Geosci.*, 1, 221–227.

Ramana, M. V., V. Ramanathan, Y. Feng, S.C. Yoon, S.W. Kim, G. R. Carmichael, and J. J. Schauer, (2010), Warming influenced by the ratio of black carbon to sulphate and the black-carbon source, *Nat. Geosci.*, DOI: 10.1038/NGEO918.

Saha, U., S. Talukdar, S. Jana, and A. Maitra, (2014), Effects of air pollution on meteorological parameters during Deepawali festival over an Indian urban metropolis. *Atmos. Env.* 98, 510-519.

Sokolik, I., and O. B. Toon, (1997), Direct radiative forcing by anthropogenic airborne mineral aerosols, *Nature*, 381, 681–683.

Stein, A. F., Draxler, R. R, Rolph, G. D., Stunder, B. J. B., Cohen, M. D., and Ngan, F., (2015). NOAA's HYSPLIT atmospheric transport and dispersion modeling system, *Bull. Amer. Meteor. Soc.*, 96, 2059-2077,

Stull, R. B., (1989), *An introduction to Boundary Layer Meteorology*, Kluwer Academic Publishers, P.O. Box 17, 3300, A A Dordrecht, the Netherland, p.620.

Talukdar, S., S. Jana, A. Maitra, and M. Gogoi, (2015), Characteristics of black carbon concentration at a metropolitan city located near land–ocean boundary in Eastern India, *Atmos. Res.*, 151, 526-514.

Tiwari, S., A. K. Srivastava, D.S. Bisht, P. Parmita, M. K. Srivastava, and S.D. Attri, (2013), Diurnal and seasonal variations of black carbon and PM<sub>2.5</sub> over New Delhi, India: Influence of meteorology, *Atmos. Res.*, 125–126, 50–62.

Weingartner, E., H. Saathoff, M. Schnaiter, N. Streit, B. Bitnar, and U. Baltensperger, (2003), Absorption of light by soot particles: determination of the absorption coefficient by means of aethalometers, *Aerosol Sci.*, 34, 1445–1463.

Yang, X., C. Zhao, J. Guo, and Y. Wang (2016), Intensification of aerosol pollution associated with its feedback with surface solar radiation and winds in Beijing, *J. Geophys. Res. Atmos.*, 121, 4093–4099, doi:10.1002/2015JD024645.

Yoon, J., J. P. Burrows, M. Vountas, W. von Hoyningen-Huene, D. Y. Chang, A. Richter, and A. Hilboll (2014) Changes in atmospheric aerosol loading retrieved from space-based measurements during the past decade, *Atmos. Chem. Phys.*, 14, 6881–6902, doi:10.5194/acp-14-6881-2014

Accepted Article